ELSEVIER

Surface Science 515 (2002) 588–596

SURFACE SCIENCE

www.elsevier.com/locate/susc

An efficient method for computing collective diffusion in a strongly interacting lattice gas

A. Serra, R. Ferrando *

Dipartimento di Fisica dell'Università di Genova, INFM and CFSBT/CNR, 1st. Naz. per la Fisica della Mater., via Dodecaneso 33, 16146 Genova, Italy

Received 15 March 2002; accepted for publication 15 June 2002

Abstract

An efficient numerical method for the calculation of the collective diffusion coefficient is developed. The method is based on the Bortz–Kalos–Lebowitz algorithm, with local updating of the particle lists for each process, coupled to the memory expansion for the calculation of the center-of-mass diffusion coefficient. The method is applied to the diffusion in a two-dimensional lattice gas model of square symmetry with repulsive lateral interactions. The numerical results are compared to two popular approximations, the Darken equation and the dynamical mean-field theory, whose respective merits are discussed. Finally, the decay of the dynamic structure factor with time is investigated.

Keywords: Diffusion and migration; Monte Carlo simulations

1. Introduction

The study of the diffusion of adatoms adsorbed on surfaces is a topic of great interest in surface science [1]. In fact, adatom mobility plays a fundamental role in many physical processes of relevant interest, like in surface chemical reactions, crystal growth, adsorption, desorption, surface melting and roughening.

If temperature is not too high, atoms deposited on the surface spend most part of their time oscillating around the adsorption sites, and sometimes jump from a site to another, with a jump frequency that depends exponentially on the activation barrier according to the Arrhenius law. The typical activation energies for diffusion are usually much lower than those for desorption, which are on the order of the eV, therefore an adatom makes many jumps on the surface before desorbing. In these conditions, the long-time motion of the adatoms is stochastic, as the time spent in each adsorption site is long enough to cancel any correlation with the previous motion. Thus, adatoms make a random walk, whose properties may be very complicated for the interactions with the other adatoms. At long times, the mean square displacement of each adatom increases linearly with time, with a proportionality constant which is, in two-dimensional isotropic systems, $4D_t$, where D_t is the single-particle (or tracer) diffusion coefficient. However, the mass transport on the surface is closely related to another diffusion

* Corresponding author. Tel.: +39-10-3536214; fax: +39-10-311066.

E-mail address: ferrando@fisica.unige.it (R. Ferrando).

0039-6028/02/$ - see front matter
PII: S0039-6028(02)02001-0

coefficient, the collective (or chemical) diffusion coefficient D_c. D_c is less simply described in terms of the elementary moves of single adatoms, but it is directly related to mass fluxes in presence of density gradients in the adsorbate (Fick's law) and, in equivalent terms, to the decay time of the long-wavelength density fluctuations at equilibrium. In fact, a density fluctuation of wave vector $\mathbf{q}$ decays as $\exp(-D_c q^2 t)$.

The collective diffusion coefficient can be obtained through different expressions. Let us consider a lattice gas of coverage θ at temperature T. The first definition relates D_c to the center-of-mass diffusion coefficient D_{CM}

$$D_c = \Theta(\theta, T) D_{CM}. \tag{1}$$

In this expression $\Theta(\theta, T)$ is the so-called thermodynamic factor, because it depends only on the static properties of the system and not on the specific kinetic model. D_{CM} can be calculated from the following expression:

$$D_{CM} = \lim_{t\to\infty} \frac{1}{4Nt} \langle |\mathbf{R}(t)|^2 \rangle, \tag{2}$$

where $\mathbf{R}(t)$ is the center-of-mass displacement

$$\mathbf{R}(t) = \sum_{i=1}^{N} [\mathbf{r}_i(t) - \mathbf{r}_i(0)] \tag{3}$$

and N is the number of particles in the system. The thermodynamic factor is related to the isothermal compressibility χ_T of the lattice gas:

$$\Theta(\theta, T) = \frac{1}{k_B T \theta \chi_T}. \tag{4}$$

On the other hand, D_c can be calculated also via the frequency-dependent dynamic structure factor $\tilde{S}_c(\mathbf{q}, \omega)$. In the lattice gas, $\tilde{S}_c$ is defined as follows. Let us consider the occupation numbers $n_\mathbf{l}$ of sites $\mathbf{l}$ in the lattice. $\tilde{S}_c$ is the Fourier transform with respect to time of the time-dependent dynamic structure factor S_c, which is the characteristic function of density fluctuations:

$$S_c(\mathbf{q}, t) = \left\langle \sum_{\mathbf{l}} [n_\mathbf{l}(t) - \theta] \exp(i\mathbf{q}\mathbf{l}) \sum_{\mathbf{m}} [n_\mathbf{m}(0) - \theta] \times \exp(-i\mathbf{q}\mathbf{m}) \right\rangle \tag{5}$$

Then D_c is recovered from $\tilde{S}_c(\mathbf{q}, \omega)$ in the limit of small wave vectors and frequencies (assuming an isotropic system):

$$D_c = \frac{\pi}{S(\mathbf{0})} \lim_{\omega\to 0} \omega^2 \lim_{q_x\to 0} \frac{1}{q_x^2} \mathscr{R}\{\tilde{S}_c(q_x, q_y = 0, i\omega)\}. \tag{6}$$

$S_c(\mathbf{0}) = S_c(\mathbf{0}, 0)$ is the static structure factor, $(1/S(\mathbf{0})) = \Theta(\theta, T)$ and $\mathscr{R}$ indicates the real part.

From the point of view of theory, the calculation of the collective diffusion coefficient is often a very cumbersome task in interacting systems. In fact, analytical (or semi-analytical) approaches, as those developed by different groups [2–5] are very difficult to apply to systems with interactions extending to more than first neighbours, and may be not reliable near phase boundaries. From the point of view of computer simulations (by the Monte Carlo method), the calculation of D_{CM} is not an easy task. It has been shown in many examples that if one applies simply the definition of D_{CM} it is very difficult to obtain reliable data, mainly because of the slow convergence of the limit in Eq. (2) [6]. This difficulty is overcome by means of the memory expansion [6]; the memory expansion allows the calculation of D_{CM} on time scales which are in many cases shorter by more than one order of magnitude with respect to the scale at which the expression in Eq. (2) reaches its asymptotic limit. This is a very important improvement, since the memory expansion allows also very easy and reliable convergency tests (see the following). However, even when the memory expansion is applied, the calculation of D_c at low temperatures may pose very difficult problems. In fact, if the Monte Carlo simulations are performed by the traditional Metropolis algorithm (or by similar algorithms), at low temperatures most of the attempted moves are rejected, and the simulation times become exponentially long with temperature.

In this paper we propose a computational method which overcomes this difficulty, combining the use of the memory expansion together with the Bortz–Kalos–Lebowitz (BKL) [7] algorithm for the Monte Carlo simulations. In this algorithm,

attempted moves are never refused, because transitions are chosen on the basis of their a priori probabilities. The method proposed here works well even at very low temperatures, where the traditional algorithm is practically useless. A Monte Carlo method for surface diffusion in interacting lattice gases based on the BKL algorithm has been presented by Bulnes et al. in Ref. [8] and applied to the calculation of the tracer diffusion coefficient in one- and two-dimensional models. They demonstrated that the BKL algorithm gives considerable improvement of the computational speed. However, the calculation of D_c is still cumbersome, and a further important speedup is achieved by the memory expansion. Another interesting Monte Carlo method for the study of D_c is the direct study of the decay of an initial long-wavelength density fluctuation (see for example Ref. [9]). Also this decay method could be implemented together with a BKL algorithm.

Here we apply our approach to the square interacting lattice gas, with the simple initial-value kinetic (IVK). This kinetic may be not realistic in many systems, however it plays the role of a reference system for testing new methods, since many data are available both from analytical calculations and Monte Carlo simulations. Here we show that in this model D_c can be studied in the full phase diagram without the massive use of parallel supercomputers, but simply by means of desktop workstations. Moreover, we present results on the dynamic structure factor, which has never been studied to our knowledge in this lattice gas. The dynamic structure factor is very important because it is proportional to the intensity in atom-scattering experiments [10].

The paper is structured as follows. In Section 2 we describe in details the computational method, and compare it to the standard Metropolis-like algorithms. In Section 3 we report the results on the thermodynamic factor, the average jump frequency and the diffusion coefficients. We compare different approximations to the exact results, and finally we show the behaviour of the thermodynamic factor near the phase boundary. In Section 4 we focus on the dynamic structure factor, and Section 5 contains the conclusions.

2. Model and computational method

As a test model for our method we choose the square lattice gas with repulsive lateral interactions. In this model, each particle interacts with its first neighbours with an interaction strength $J > 0$. Moreover, we make a strong assumption about the kinetics, by adopting the so-called IVK, in which the barrier of a given jump process is determined only by the initial configuration (i.e. by the configuration before the jump). In fact, in the IVK, the barrier for a given jump is calculated adding to the bare diffusion barrier, a contribution $-J$ for each occupied neighbour in the position before the jump. Even if the IVK obeys to the detailed balance (and therefore the thermodynamic properties as calculated by the IVK are correct), it cannot be considered a reliable model for the kinetics in real systems, except for those systems where interactions are strictly limited to the first neighbours (see the discussion in [2]). However we choose this kinetics as a test model for our algorithm, because many analytical and numerical results already exist in literature [2,3, 11,12]. Finally, we limit the extension of particle jumps to first-neighbour sites, thus neglecting the possibility of long jumps [13].

The repulsive square lattice gas presents an ordered phase (with degeneracy two) at low temperatures and medium coverages. A schematic representation of the phase diagram of the square lattice gas with nearest neighbour repulsion is given in Fig. 1.

The BKL-like algorithm [7,14] adopted in our simulations can be described as follows. Let us consider a configuration C in the lattice gas. We can subdivide all possible processes in C in different classes, in such a way that processes belonging to a given class are equivalent. In our case, we put in the same class all processes with the same activation barrier. There are four different possible activation barriers E_s ($s = 1, 2, 3, 4$) in the square lattice gas with the IVK. E_s is associated with a jump process whose initial configuration has $s - 1$ first neighbours occupied: therefore $E_s = E_0 - (s - 1)J$, where E_0 is the bare activation barrier for an isolated particle. In general, in a configuration C, $n_s(C)$ processes of class s are possible. A weight

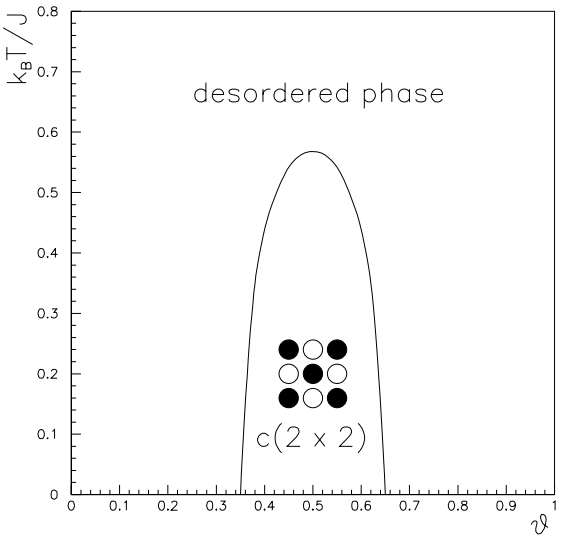

Fig. 1. Schematic representation of the phase diagram of the square lattice gas with nearest-neighbour repulsion J. The critical temperature T_c at coverage $\theta = 0.5$ is given by $J/(k_B T_c) \simeq 1.76$.

p_s is associated to each individual process; p_s is the same for all processes in class s and it is given by

$$p_s = v_s \exp\left(-\frac{E_s}{k_B T}\right). \tag{7}$$

For simplicity, we take all $v_s = v$, and consider as a elementary time constant the quantity $\tau_0 = v^{-1}\exp[E_0/(k_B T)]$. The individual weights are summed up to give the total weight $P(C)$:

$$P(C) = \sum_{s=1}^{4} n_s(C) p_s, \tag{8}$$

together with the partial weights $P(l;C)$

$$P(l;C) = \sum_{s=1}^{l} n_s(C) p_s. \tag{9}$$

By definition, $P(4;C) = P(C)$ and $P(0;C) = 0$. After having calculated the weights, a move is chosen among the possible ones according to its individual weights. First, a random number r, with $0 < r \leqslant P(C)$ is chosen. If $P(l-1;C) < r \leqslant P(l;C)$, class l is selected. Then an integer random number i is chosen such that $1 \leqslant i \leqslant n_l(C)$: then the ith event of class l is performed. In order to fulfill the detailed balance condition, time is advanced by the quantity $\delta t(C)$, extracted from the time-interval exponential distribution with average lifetime $\tau_0/P(C)$.

The advantage of this algorithm with respect to the traditional Metropolis-like schemes [11] is that no moves are refused. In the traditional schemes, many refusals are obtained at low temperatures or at high coverages, with subsequent waste of computer time. On the other hand, the BKL algorithm needs the calculation of the weights at each step, and this calculation could imply in principle a loop on all particles in the system, to update the lists of particles which belong to any given class. However, a local updating is possible, such that the lists are not recalculated from the beginning at each move, but they are modified only for what concerns the particle which made the move and its local environment. This local updating speeds up the program by orders of magnitude. We have compared the speed of the BKL algorithm to that of the Metropolis-like algorithm in the case of high temperatures (no lateral interactions) at different coverages, computing the tracer diffusion coefficient to a given degree of accuracy. At low coverages both algorithms require more or less the same computer time; on the other hand, at $\theta \simeq 0.9$ the BKL algorithm is about 5 times faster. We remark that this happens already at high temperature; at lower temperatures, the Metropolis scheme requires an exponentially increasing computer time, while the efficiency of the BKL algorithm does not change strongly. For example, at $\theta = 0.5$ and $\beta J = 2.41$, the BKL algorithm is about 400 times faster.

Finally, a brief comment on the use of this algorithm in systems where interactions involve more distant neighbours. In these systems, there can be a huge number of classes of different processes, and the implementation of the algorithm may become cumbersome. However, in this case it can be more convenient to associate to each atom a weight, calculated by summing up the weights which are associated to its possible moves to its nearest neighbours. Then atomic weights can be collected by a binary-tree procedure [15].

3. The diffusion coefficient

3.1. Thermodynamic factor

The thermodynamic factor can be numerically calculated in two ways, both based on grandcanonical Monte Carlo simulations at fixed chemical potential μ. The first exploits the relation [2,16]:

$$S(\mathbf{0}) = k_B T \frac{\partial \ln \theta}{\partial \mu}. \tag{10}$$

The second method follows from the relation between $S(\mathbf{0})$ and the fluctuations in the particle number N:

$$S(\mathbf{0}) = \frac{\langle N^2 \rangle - (\langle N \rangle)^2}{\langle N \rangle}. \tag{11}$$

The first method converges very fast if one is treating system parameters which are not close to the phase boundary: there, it is easy to have a fast convergence on the average value of θ in the grandcanonical simulation. Moreover, the dependence of θ on μ is rather smooth in this case, and numerical derivatives are easy to calculate. The second method is more convenient when the phase-diagram region that is very close to the phase boundary is studied. There, fluctuations are large and numerical derivatives become less reliable.

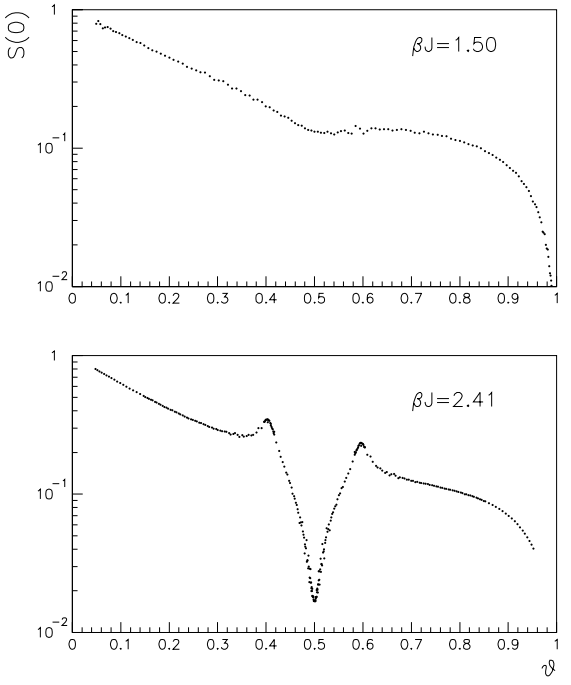

Fig. 2. $S(\mathbf{0})$ as a function of the coverage at two different temperatures, above and below T_c. The results are obtained on a system size of 60×60.

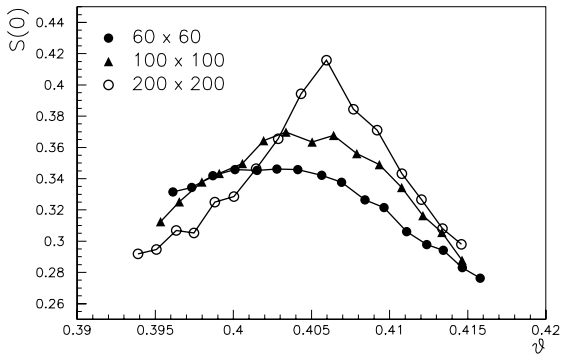

Fig. 3. $S(\mathbf{0})$ at $\beta J = 2.41$ around the phase boundary for different sizes of the system.

The results for $S(\mathbf{0})$ as a function of θ at two different temperatures (above and below the critical temperature) are given in Fig. 2. The numerical results are obtained on a system size of 60×60 sites by Eq. (10), and are in very good agreement with those obtained by the cluster variation method (CVM) [2,3] except for the region around the two maxima in the lower panel. In fact, these maxima are close to the phase boundary, and there, $S(\mathbf{0})$ diverges in this model [12]. The divergence of $S(\mathbf{0})$ at the phase boundary can be studied by simulating systems of larger and larger sizes. The results are reported in Fig. 3, where sizes up to 200×200 are considered. The points in Fig. 3 are obtained by Eq. (11) on a desktop workstation within a reasonable computer time.

3.2. Average jump frequency, tracer diffusion coefficient and center-of-mass diffusion coefficient

As underlined in Section 1, the most difficult quantity to calculate in order to get the collective diffusion coefficient D_c is the center-of-mass diffusion coefficient D_{CM}. On the other hand, both the average jump frequency $\langle w \rangle$ [2,3] and the tracer diffusion coefficient D_t, defined as

$$D_{\mathrm{t}} = \lim_{t\to\infty} \frac{1}{4Nt} \sum_{i=1}^{N} \langle [\mathbf{r}_i(t) - \mathbf{r}_i(0)]^2 \rangle, \tag{12}$$

are rather easily obtained by MC simulations. Therefore, it is tempting to try to approximate D_{CM} by means of these quantities. This leads to two different approximations:

(a) $D_{\mathrm{CM}} = D_{\mathrm{t}}$; this is the so-called Darken equation (DE) [16],
(b) $D_{\mathrm{CM}} = a^2\langle w \rangle$; this is known either as generalized DE [17] or equivalently dynamical mean-field theory (DMFT) [18].

In the DE approximation, the memory effects on D_{CM} are taken into account by approximating them by the memory effects on D_{t}. Since the memory effects contribute to slow down the diffusion coefficient, and they are stronger on D_{t} than on D_{c} [2,18–20], we expect the DE to give an underestimate of D_{CM}. On the other hand, in the DMFT the memory effects on D_{CM} are neglected. This is exact in the limit of very high temperatures, and leads to an overestimate of D_{CM}. In the following we compare the exact results for D_{CM} to those of both approximations.

The most efficient way to compute numerically the exact expression for D_{CM} (Eq. (2)) is the memory expansion, introduced by Ying et al. in Ref. [6]. In the memory expansion one subdivides time into intervals of length τ ($t_m - t_{m-1} = \tau$) and writes D_{CM} as

$$D_{\mathrm{CM}} = \frac{1}{4N\tau}\left[C(0) + 2\sum_{k=1}^{\infty} C(k\tau)\right], \tag{13}$$

where

$$C(k\tau) = \langle \delta\mathbf{R}(t_m)\delta\mathbf{R}(t_m + k\tau)\rangle, \tag{14}$$

with $\delta\mathbf{R}(t_m) = \mathbf{R}(t_m) - \mathbf{R}(t_{m-1})$. The convergence of the memory expansion at $\beta J = 1$ and $\theta = 0.5$ is shown in Fig. 4, where two different values of τ were used.

In Fig. 5 we compare D_{CM} as obtained from the memory expansion to the DE and DMFT approximations, at two different βJ, one above and one below the critical temperature. It is evident that the DMFT approximation is very good in the region of the phase diagram where a disordered phase is present, for example at any coverage at $\beta J = 1$ and at low or high coverages at $\beta J = 2.41$. The DMFT clearly overestimates D_{CM} when the ordered phase is present, and memory effects become important in slowing down the diffusive motion. On the other hand, the DE approximation is not accurate in presence of the disordered phase (except for very low coverages), while it is good in presence of the ordered phase. This indicates that, in this model, and with this kinetics, collective and single-particle memory effects are nearly of the same magnitude in the ordered phase. As expected, D_{CM} lies always between the DE and DMFT approximations, that can be considered respectively lower and upper limits to the exact result.

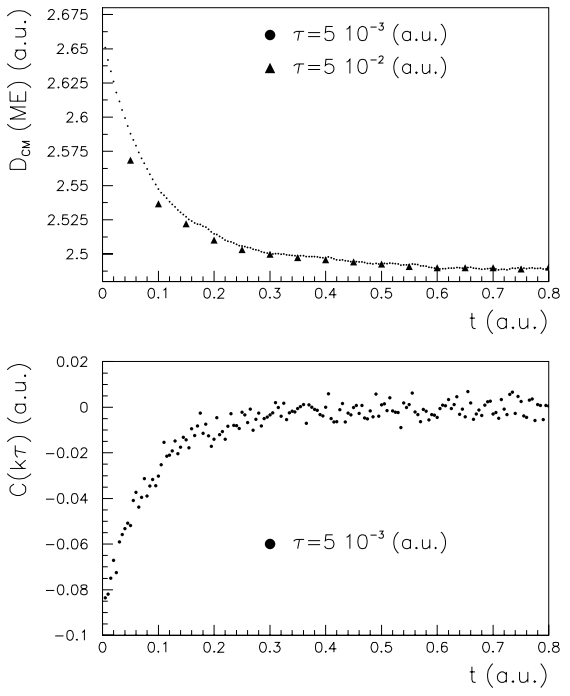

Fig. 4. Convergence of the memory expansion for $\beta J = 1$ and $\theta = 0.5$ for different values of the discretization interval τ.

The above results seem to indicate that DE and DMFT approximations are complementary, the DMFT being preferred outside the phase boundary and the DE inside. However some care should be taken to generalize the above results to different models or kinetics. In fact, we could expect the DMFT to be a reasonable approximation in any

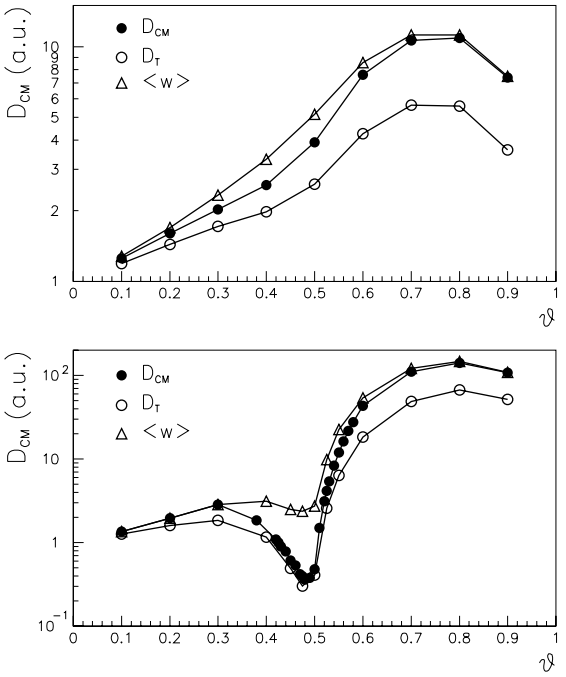

Fig. 5. Comparison of D_{CM}, D_t and $\langle w \rangle$ as functions of the coverage for temperatures above and below T_c.

model in the region outside the phase boundary (because there are exact results insuring that collective memory effects disappear at high temperatures and at low coverages). On the contrary, we have at the moment no reason to believe that collective and single-particle memory effects to be nearly the same in any model in the region inside the phase boundary, and therefore the accuracy of the DE is not insured there, and care must be taken in generalizing the results of the present model to other cases.

3.3. Collective diffusion coefficient

As said in Section 1, the collective diffusion coefficient is calculated by means of the product of the thermodynamic factor and of the center-of-mass diffusion coefficient (see Eqs. (1)–(4)). The results are shown in Fig. 6, where data above and below the critical temperature are shown. The results are in good quantitative agreement with those obtained previously by the CVM [2,3]. Some differences are found only in the case below the

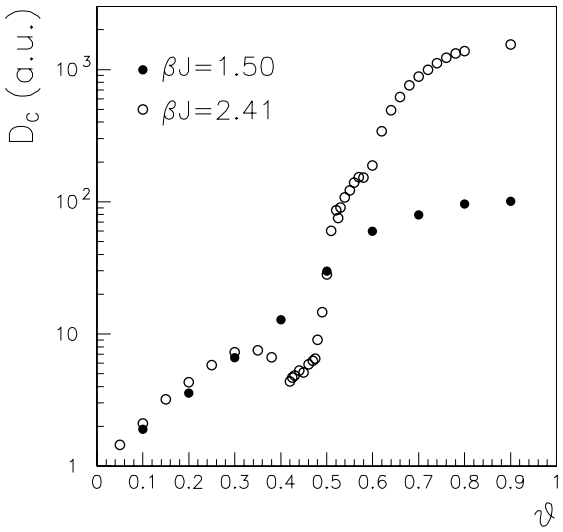

Fig. 6. Collective diffusion coefficient D_c as a function of the coverage θ at two different temperatures: above (•) and below (○) the critical temperature.

critical temperature. In fact, the CVM calculations showed that after the minimum slightly below $\theta = 0.5$, there is a steep increase leading to a very narrow local maximum; this narrow local maximum (which was indeed found even more clearly in older Monte Carlo calculations [11]) is not reproduced by the present Monte Carlo calculations, which indicate that it is probably an artifact due to an overestimate of the peak of the thermodynamic factor at $\theta = 0.5$.

4. Dynamic structure factor

The dynamic structure factor $S_c(\mathbf{q}, t)$, defined in Eq. (5), has a quite simple form if memory effects are neglected [2]. In this approximation, $S_c(\mathbf{q}, t)$ has an exponential decay at all times for each $\mathbf{q}$:

$$S_c(\mathbf{q}, t) = S(\mathbf{q}) \exp\left[-\Omega_c^0(\mathbf{q}) t \right], \tag{15}$$

where $\Omega_c^0(\mathbf{q})$ is the frequency function, given by

$$\Omega_c^0(\mathbf{q}) = \frac{\langle w \rangle}{S(\mathbf{q})} \sum_{\mathbf{a}} [1 - \exp(\mathbf{q} \cdot \mathbf{a})], \tag{16}$$

where the sum is extended to the nearest neighbours $\mathbf{a}$ of the site $\mathbf{0}$. When memory effects are included, $S_c(\mathbf{q}, t)$ has a more complex form, but we

could expect that at long times, again the exponential decay is recovered, so that, at $t \to \infty$

$$S_c(\mathbf{q},t) \simeq \gamma(\mathbf{q}) \exp[-\alpha(\mathbf{q})t]. \quad (17)$$

This guess is confirmed by our numerical data reported in Figs. 7 and 8; the asymptotic decay is always exponential, but at short times, and especially in the case of low temperatures, the initial decay is even faster than the asymptotic exponentials. Because of that, the extraction of the decay function $\alpha(\mathbf{q})$ of Eq. (17) is meaningful: $\alpha(\mathbf{q})$ is the half width at half maximum of the quasi-elastic peak of the time Fourier transform of $S_c(\mathbf{q},t)$. This quantity is measured in helium-atom and neutron scattering experiments [10,21]. The results at $\beta J = 2.5$ and $\theta = 0.5$ are reported in Fig. 9, both along the x direction (full circles) and the diagonal direction (open circles) for $\mathbf{q}$ up to the border of the first Brillouin zone. Along the x direction, $\alpha(\mathbf{q})$ increases monotonically, reaching its maximum at the zone border. This is qualitatively the same behaviour of the case of $\beta J = 0$. On the contrary, along the diagonal direction, there is a minimum at the zone border. This minimum is due to a maximum in $S(\mathbf{q})$ (see Eq. (16)) which appears only when there is the low-temperature ordered

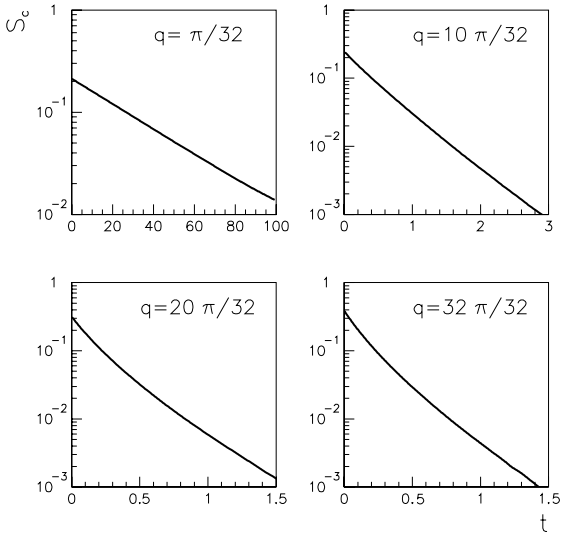

Fig. 7. $S_c(\mathbf{q},t)$ at $\beta J = 1$ and $\theta = 0.5$ for different values of $\mathbf{q}$ along the x direction. The decay is asymptotically exponential, and even at short times, there are only slight deviations from the exponential behaviour.

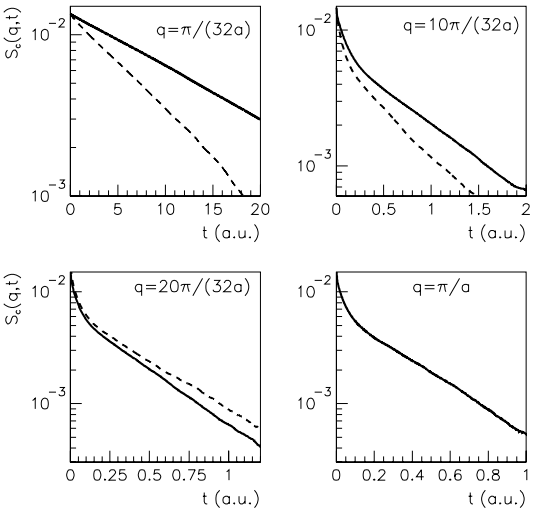

Fig. 8. $S_c(\mathbf{q},t)$ at $\beta J = 2.5$ and $\theta = 0.5$ for different values of $\mathbf{q}$ along the x direction (—) and along the diagonal direction (- - -). The decay is asymptotically exponential, but at short times and large $\mathbf{q}$, the deviations from the exponential behaviour are evident.

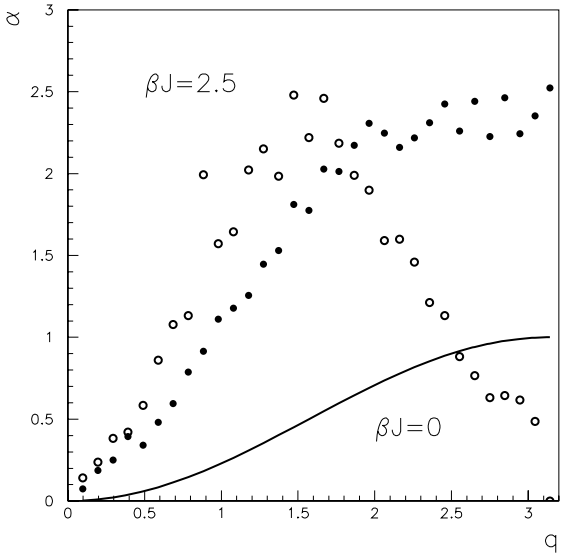

Fig. 9. Asymptotic decay function $\alpha(\mathbf{q})$ of $S_c(\mathbf{q},t)$ (see Eq. (17)) at $\beta J = 2.5$ and $\theta = 0.5$, along the x direction (•) and along the diagonal direction (○). The full line corresponds to the results in the absence of lateral interactions along the x direction.

phase; this maximum corresponds to a diffraction peak from the $c(2 \times 2)$ phase. At high temperatures, the maximum in $S(\mathbf{q})$ along the diagonal

direction disappears, and therefore the same happens to the minimum in $\alpha(\mathbf{q})$.

5. Conclusions

In this paper we have investigated the collective diffusion in a lattice-gas model on square symmetry with repulsive nearest-neighbour interactions by means of Monte Carlo simulations. We have developed an efficient algorithm to investigate the low-temperature properties of the model. This algorithm, which is based on the classical BKL scheme [7], allows a speedup of several orders of magnitude compared to the usual Metropolis-like algorithms. Moreover, in order to optimize the numerical evaluation of the diffusion coefficients, which usually involves the calculation of asymptotic slopes, the memory expansion [6] has been adopted. By means of these methods, precise numerical data have been obtained by a modest computational effort on desktop workstations.

The main results obtained in this paper are three. The first one concerns the comparison of the exact results with two rather popular approximations, the DE and the DMFT. We have shown that the former overestimates the memory effects, thus underestimating the collective diffusion coefficient. On the contrary, the latter neglects the memory effects, overestimating the diffusion coefficient. In this way, one can give lower and upper limits to D_c by means of quite simple approximations which do not involve the calculation of the cumbersome D_{CM}. In our model, it turns out that the DMFT is more accurate in the disordered region of the phase diagram, while it seems that the DE gives better estimates in the ordered region.

The second result concerns the precise calculation of D_c at low temperatures in order to verify whether there is a local maximum just at half coverage, as it was obtained by previous CVM calculations [2], and by Monte Carlo simulations [11]. Here we have not found any local maximum.

The third result is the investigation of the dynamic structure factor, and especially of its decay with time. We have found that the dynamic structure factor decays asymptotically with time as an exponential. At short times, there are deviations from the exponential decay which are more pronounced at low temperatures and large $\mathbf{q}$. Moreover, we have investigated the decay function $\alpha(\mathbf{q})$, which, when ordering is present, shows additional minima along the diagonal direction in reciprocal space at the Brillouin zone boundary.

References

[1] T. Ala-Nissila, R. Ferrando, S.C. Ying, Adv. Phys. 51 (2002) 949.
[2] A. Danani, R. Ferrando, E. Scalas, M. Torri, Int. J. Mod. Phys. B 11 (1997) 2217.
[3] A. Danani, R. Ferrando, E. Scalas, M. Torri, Surf. Sci. 409 (1998) 117.
[4] A.V. Myshlyavtsev, V.P. Zhdanov, Surf. Sci. 291 (1993) 145.
[5] Z. Chvoj, H. Conrad, V. Chab, Surf. Sci. 376 (1997) 205; Z. Chvoj, J. Phys. CM 12 (2000) 2135.
[6] S.C. Ying, I. Vattulainen, J. Merikoski, T. Hjelt, T. Ala-Nissila, Phys. Rev. B 58 (1998) 2170.
[7] A.B. Bortz, M.H. Kalos, J.L. Lebowitz, J. Comp. Phys. 17 (1975) 10.
[8] F.M. Bulnes, V.D. Pereyra, J.L. Riccardo, Phys. Rev. E 58 (1998) 86.
[9] M.A. Zaluska-Kotur, S. Krukowski, L.A. Turski, Surf. Sci. 441 (1999) 320.
[10] J.W.M. Frenken, B.J. Hinch, J.P. Toennies, Ch. Wöll, Phys. Rev. B 41 (1990) 938.
[11] C. Uebing, R. Gomer, J. Chem. Phys. 95 (1991) 7626.
[12] A.V. Myshlyavtsev, A.S. Stepanov, C. Uebing, V.P. Zhdanov, Phys. Rev. B 52 (1995) 5977.
[13] R. Ferrando, R. Spadacini, G.E. Tommei, Phys. Rev. E 48 (1993) 2437.
[14] M. Kotrla, Comp. Phys. Comm. 96 (1996) 82.
[15] C. Mottet, R. Ferrando, F. Hontinfinde, A.C. Levi, Eur. Phys. J. D 9 (1999) 561.
[16] R. Gomer, Rep. Prog. Phys. 53 (1990) 917.
[17] R. Ferrando, E. Scalas, M. Torri, Phys. Lett. A 186 (1994) 415.
[18] T. Hjelt, I. Vattulainen, J. Merikoski, T. Ala-Nissila, S.C. Ying, 380 (1997) L501.
[19] I. Vattulainen, J. Merikoski, T. Ala-Nissila, S.C. Ying, Phys. Rev. B 57 (1998) 1896.
[20] I. Vattulainen, S.C. Ying, T. Ala-Nissila, J. Merikoski, Phys. Rev. B 59 (1999) 7697.
[21] M. Bienfait, J.M. Gay, H. Blank, Surf. Sci. 204 (1988) 331.